Chapter 6

Synthesis of Mg/MnO_2 and Mg/CuO catalyst and its application in synthesis of glycerol carbonate: Establishing role of support metal in glycerol conversion

6.1. Introduction

The need for energy is continuously rising due to the tremendous population growth and technological advancement occurring globally. The biodiesel industry has grown significantly in recent years in response to the current energy demand. A surplus of crude glycerol (about 10% of the overall output) is produced during the manufacturing of biodiesel as a substitute for fossil fuels. The excess glycerol mostly hurts the biodiesel companies' ability to compete on the market. Given all of these concerns, recent research has focused on the efficient and sustainable conversion of crude glycerol into a variety of value - added products. Glycerol carbonate is one of the most desirable glycerol derivatives due to its exceptional physicochemical qualities, which include low flammability, water solubility, and high biodegradability. In this chapter, we constructed solid base catalysts made of magnesium, such as Mg/CuO and Mg/MnO_2, and used them to transesterify glycerol. However, combining magnesium with transition metal oxides like manganese oxide and copper oxide to increase the stability, catalytic activity of MgO was both intriguing and difficult. The effect of transition metals like Mn and Cu on the activity of magnesium metal in glycerol transesterification has also been explored in this study. Here, a number of co-precipitation produced transition metal oxide (Cu and Mn) catalysts were produced for application in the production of glycerol carbonate. Individual reactions were monitored, and the effectiveness of these catalysts and the conversion rate of glycerol were both thoroughly investigated. Systematic analysis was done on the correlation between reactant species conversion, product yield percentage, selectivity, and acidic and basic characteristics. A variety of characterization methods, including XRD, TGA-DSC, FTIR, TEM and XPS spectra, were used to determine the physicochemical characteristics of the proposed catalyst and their impact on catalytic performance.

6.2. Synthesis of Mg modified transition metal catalysts

The co-precipitation method was used to create magnesium and transition metal-based catalysts, such as Mg/CuO and Mg/MnO_2, within a constant pH range of 8 – 10. In the beginning, the necessary quantity of magnesium nitrate was taken in a beaker and dissolved in a certain quantity of double distilled water. A precise quantity of manganese nitrate was taken and dissolved in double distilled water in a different beaker. At 40 ℃, both solutions were combined and stirred (Mg:Mn molar ratio equal to 1:2 in the reaction mixture). Ammonia solution (ammonium hydroxide) was added dropwise during the reaction process to maintain the pH between 8 and 10, as well as to create precipitation. The reaction mixture was agitated for an additional 5 hours after the precipitate had formed in order to promote the precipitate phase's selective growth. After filtering, the product combination was repeatedly rinsed in hot water to eliminate any remaining contaminants. The solid sample was then calcined at 400°C for 5 hours in a muffle furnace after spending the previous day at 110°C in an oven. The final step was to remove the finished product from the furnace, smash it, and screen it to obtain the fine powder form of the catalyst. The acquired catalyst was kept in a safe place before being utilised to transesterify glycerol. Similar to this, glycerol transesterification catalysts like Mg modified CuO were created and tested.

6.3 Characterization of synthesized catalyst

6.3.1 TGA study

The thermal stability of the catalyst was assessed using TGA and DSC, and the precursors' annealing temperature was established. Figure 6.1(a) depicts, respectively, the temperature profiles of the precursors MMO and CMO. Figure. 6.1(a) clearly shows three areas of weight loss in the MMO sample. The weight loss observed i.e., 6.224%, which is caused by removal of lattice crystal moisture. The DSC plot shows that the process is exothermic in nature with the heat flow of -212.5696 J/g. This result is consistent with the previous studies [175, 176].

There has been a slight weight loss throughout the temperature range. The TG curve exhibits no weight loss further, indicating that the sample has stabilised. Figure 6.1(b) shows that of Mg/CuO (CMO). The graph shows two stages of weight loss. First stage of weight loss is from room temperature to 270 ℃ due to removal of surface absorbed water and another is from 300 to 700 ℃ due to breaking and formation of bonds between Cu and Mg. The DSC graph shows the process is endothermic in nature and the heat flow during first stage of weight loss is 472.3123 J/g at 244.50 ℃ [177].

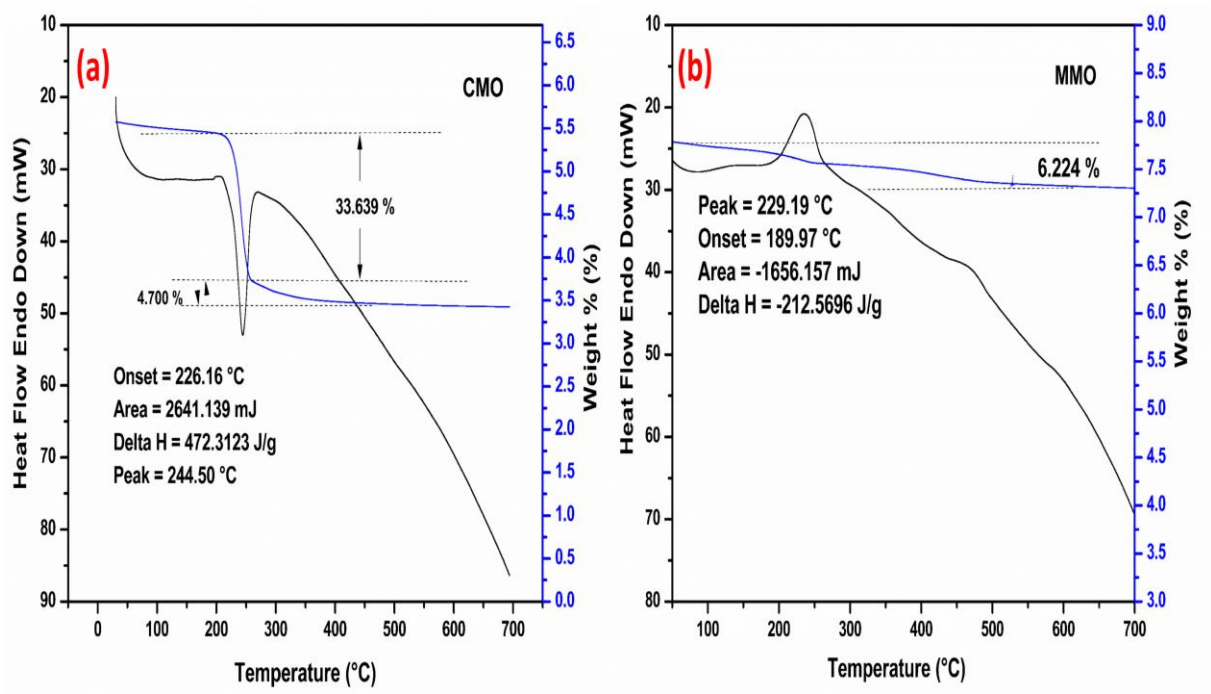

Figure 6.1. TGA-DSC of (a) CMO and (b) MMO.

6.3.2 XRD analysis

Figure 6.2 shows the XRD diffraction pattern of CMO. The diffraction peaks appeared at 2θ equal to 35.88, 39.00, 49.00, 58.57 shows the formation of $MgCu_4O_5$ matched with JCPDS card no. 470681. The remaining peaks at 2θ values 32.76, 61.63, 65.99, 65.99, 72.00, 75.55 shows the existence of CuO in the crystal lattice matched with JCPDS card no. 010720629. This confirms the formation of mixed phase of $MgCu_4O_5$ and CuO in CMO catalyst [177]. On the other hand, Figure 6.2 shows the XRD pattern of MMO. It is clearly visible in the diffraction

patterns consisting of miller indices at (101), (200), (103), (211), (202), (220), (303), (215), (116), and (323) corresponds to 2θ = 18°, 29°, 32°, 36°, 37°, and 44°, 56°, 61°, 64°, and 66°, which resembles to $MgMn_2O_4$ spinel crystal structure, 141/amd space group, the crystal system is tetragonal with lattice parameters a = b = 5.7280, c= 9.3460. all angles α = β = γ = 90º [178] consistent with JCPDS file no. 0230392, respectively. The high degree of crystallinity of the materials is indicated by the strong peak in XRD patterns. The structure of $MgMn_2O_4$ is similar to the spinel tetragonal structure, in which Mg^{2+} and Mn^{3+} /$^{4+}$ ions occupy tetrahedral and octahedral positions, respectively.

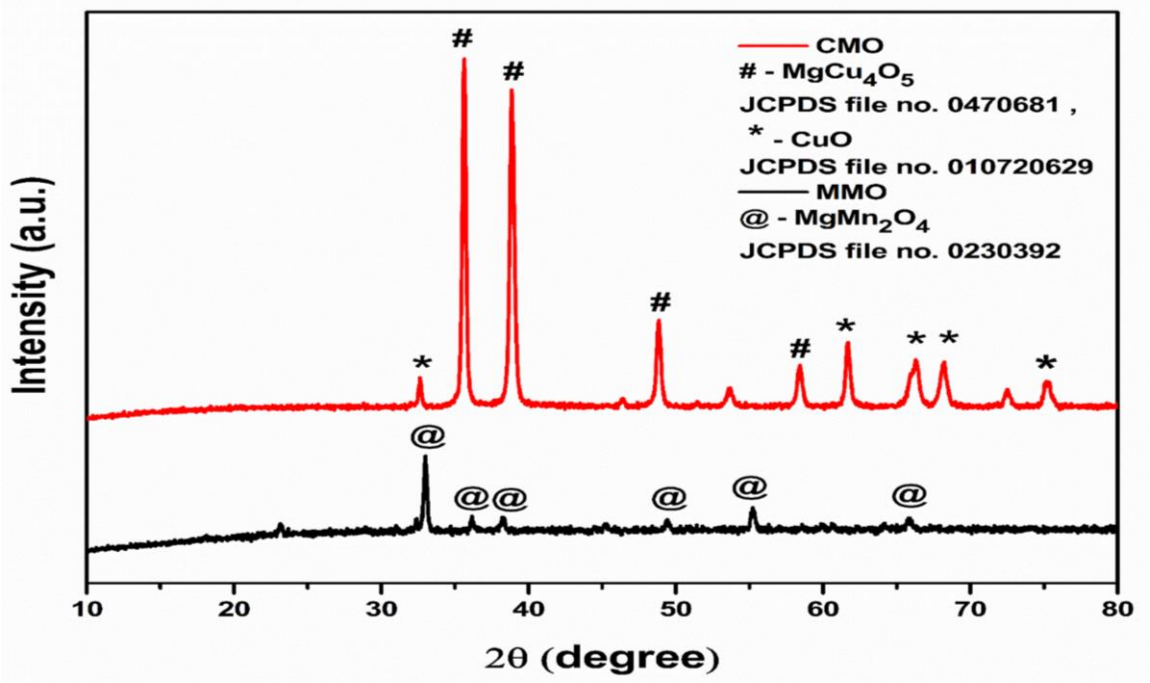

Figure. 6.2. XRD patterns of MMO and CMO.

6.3.3 XPS analysis

The oxidation states and the atomic energy level of the different elements present in the synthesized catalyst MMO and CMO are investigated through XPS analysis depicted in Figure. 6.3 (a) and (b). The XPS characteristics peaks were calibrated considering the adventitious C1s peak as the reference showing binding energy at 284.68 eV. In Figure 6.3 (a), the survey spectra show the existence of Mg, Mn and O in the prepared MMO catalyst. In the magnesium

spectrum, the characteristics peak appear at 1303.79 eV shows the existence of Mg metal present in 1s shell having +2 oxidation state. The Mn spectrum shows Mn 2p peak seems at binding energies 641.30 eV resembles Mn $2p_{3/2}$, 652.82 eV corresponds to Mn $2p_{1/2}$ shows the presence of Mn in +4 and +3 oxidation state [179]. In the O1s spectrum, the characteristic peak at 530.92 eV and 529.38 eV is due to Mn-O and Mg-O metal-oxygen bonding [180, 181]. Figure 6.3 (b), shows the survey spectra of CMO catalyst which confirms the existence of Mg, Cu and O in the CMO catalyst. In magnesium spectrum, the characteristic peak at 1303.79 eV confirms the presence of Mg metal in 1s shell with +2 oxidation state. The Cu XPS spectrum shows Cu in 2p shell having binding energies 933.55 eV signifies Cu $2p_{3/2}$, the decovoluted peaks at binding energies 941.41, 943.53 eV signifies presence of strong Cu^{+2} satellite peak. Also, the peaks at 953.52, 962.23 eV shows $Cu2p_{1/2}$ depicts the presence of strong Cu^{+2} satellite peak. The O1s spectra shows the peaks at 529.43, 531.39 eV confirms the metal oxygen bonding [182, 183, 184]. The outcomes are in agreement with the Thermo Fisher XPS database and NIST XPS database. The oxidation states of the existing elements display confirmation with the XRD results.

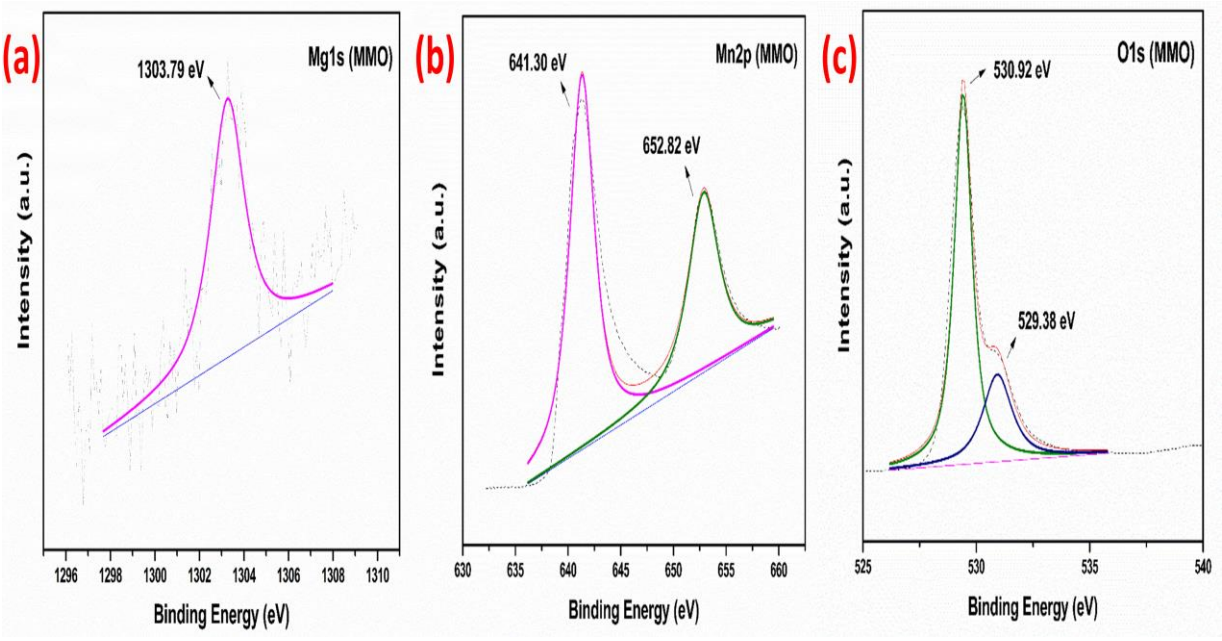

Figure. 6.3 (A). XPS Spectra of MMO.

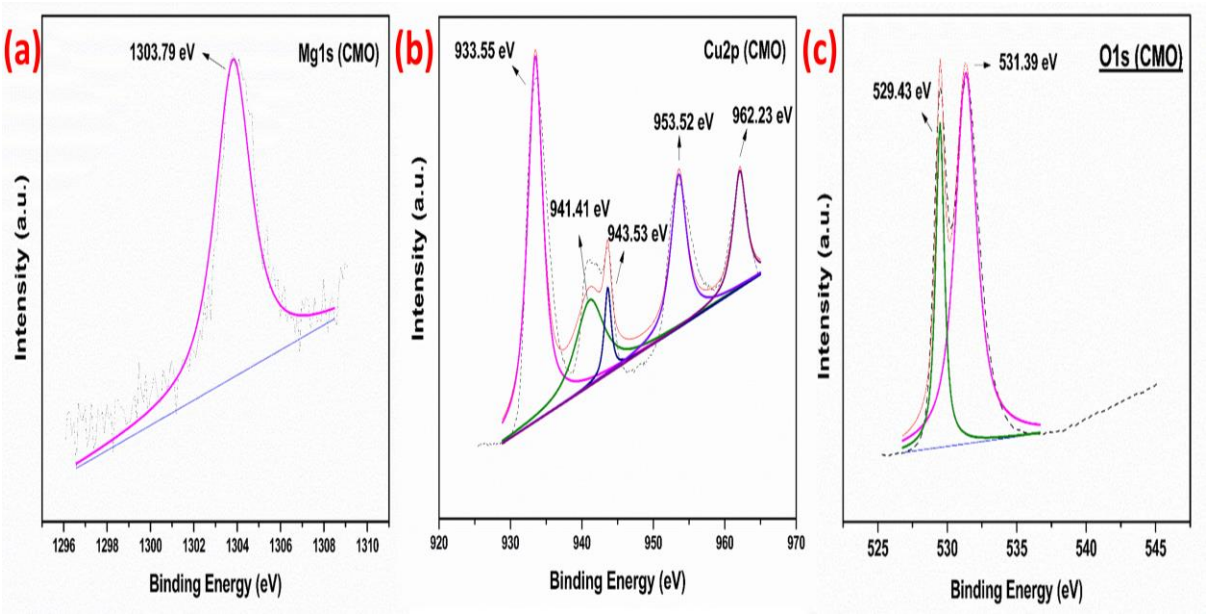

Figure 6.3 (B). XPS Spectra of CMO.

6.3.4 FTIR spectra

Figure.6.4 shows the FT-IR patterns of MMO and CMO respectively. The peaks appeared between 500 to 650 cm^{-1} denotes the metal – metal and metal oxygen bonding. The two distinct peaks at 536 cm^{-1} and 634 cm^{-1} corresponds to Mn-O and Mg-O vibrations respectively [185, 175, 176]. In CMO, the vibration band at 524.48 and 590.37 cm^{-1} corresponds to Mg-O and Cu-O. The small peak around 1600 cm^{-1} depicts the bending vibration of adsorbed water molecules in the crystal lattice. Further, the peak appeared at 3400 to 3700 cm^{-1} signifies the stretching vibration of water and hydroxyl molecules present in the crystal lattice due to absorption of water [186, 187].

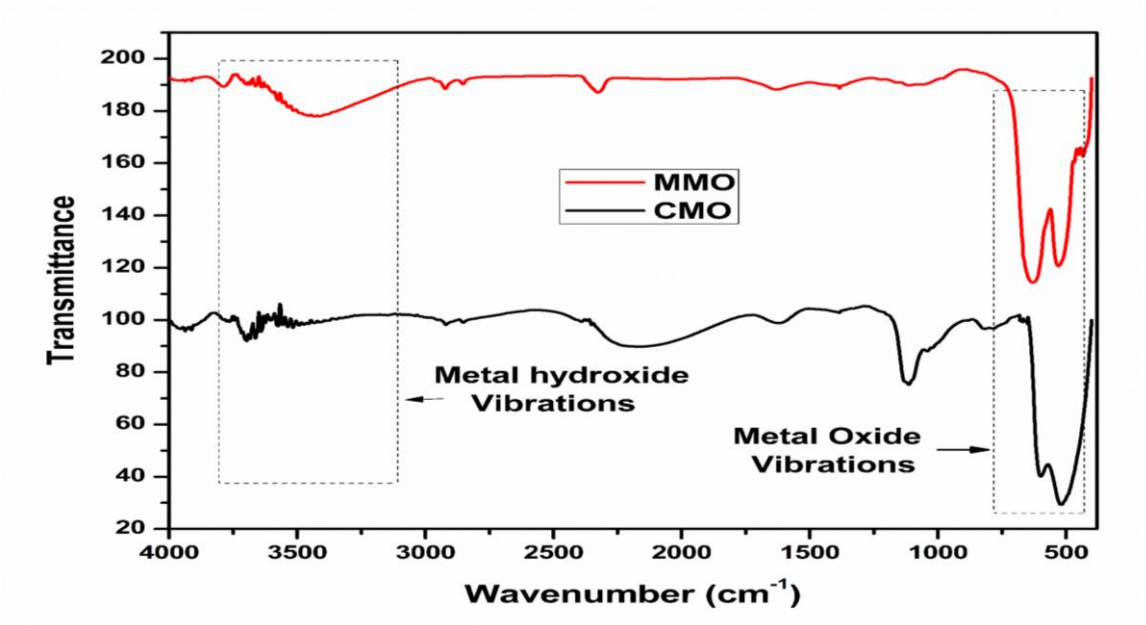

Figure 6.4. FT-IR spectra of MMO and CMO respectively.

6.3.5 TEM analysis

The TEM micrographs of MMO were studied under 100 nm resolution. The micrographs show the particles are of irregular spheroidal morphology. Two types of particles were seen which collaborates to the Mn and Mg particles adsorbed one over the other. The selected area diffraction pattern (SAED) shows clearly defined electron diffraction spots substantiate the crystalline nature of the MMO spinel. The interplanar spacing between crystal planes were calculated by high resolution TEM micrograph. The interplanar d spacing comes out to be 1.87 A^{o} which is consistent with crystal plane (301). The EDAX pattern confirms the presence of different elements in their respective atomic % which is Mg in 18.92%, Mn in 47.48 % and O in 33.61% [188, 189].On the other hand, the TEM micrograph of CMO shows that particles are of spherical as well as rectangular morphology stick to each other. The selected area diffraction pattern (SAED) depicts electron diffractions spots clearly visible evident the crystalline nature of CMO catalyst. The EDAX pattern confirms the presence of different elements in their respective atomic % which is Mg in 17.82 %, Cu in 38.56 % and O in 43.62 % [190] .The result is in consistent with the XRD results.

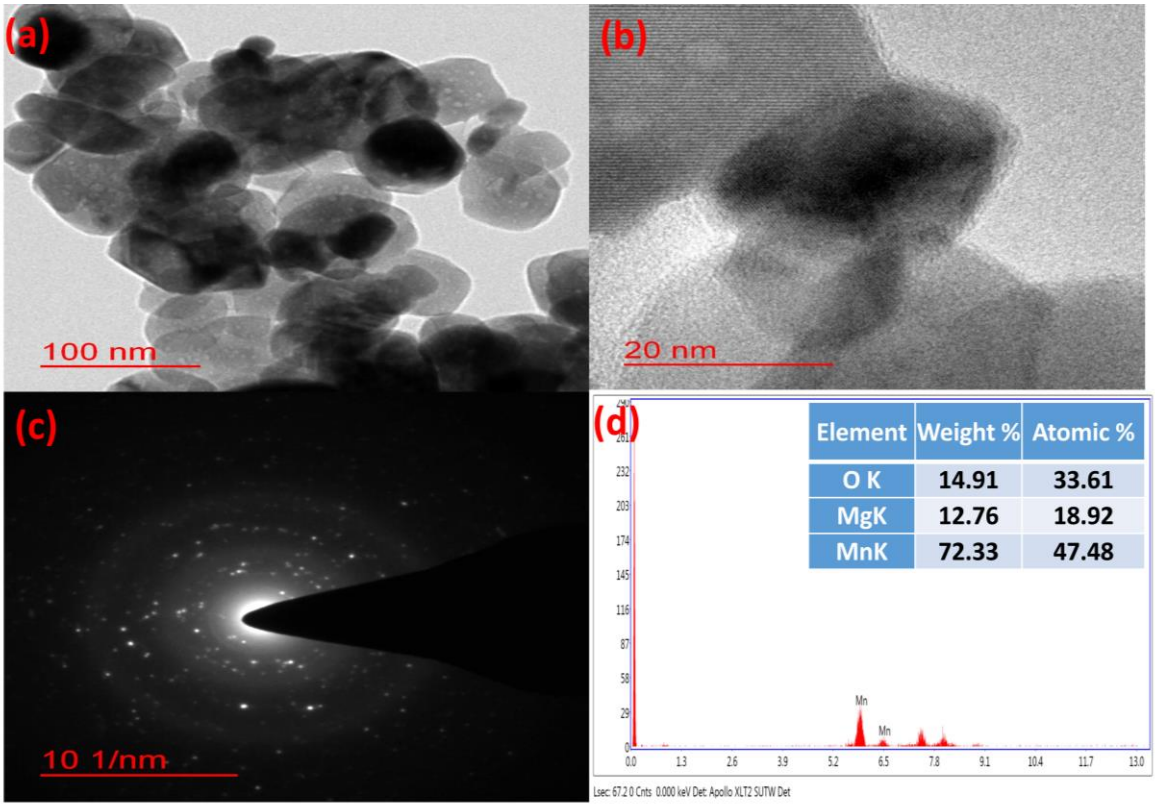

Figure 6.5 (A) TEM micrographs of MMO.

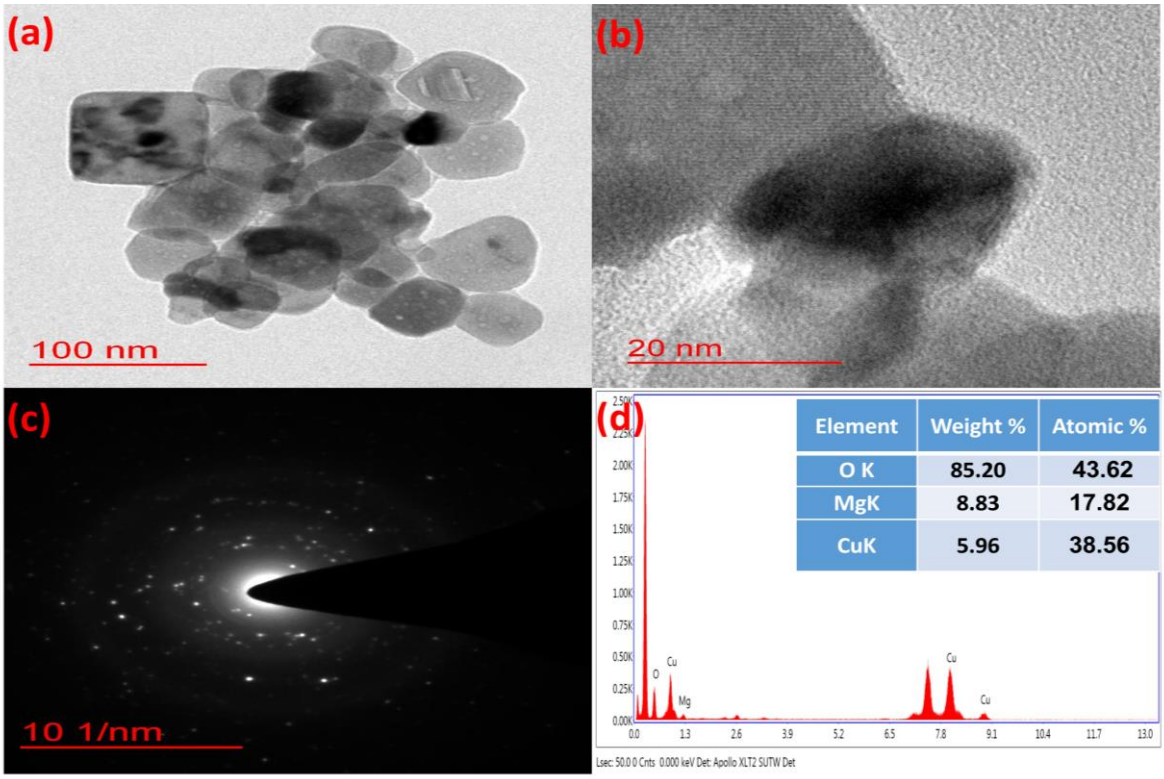

Figure 6.5 (B). TEM micrographs of CMO.

6.3.6 Basicity

In order to trans esterify glycerol, a heterogeneous catalyst's basic site and basicity play a significant role, thus it is imperative to research the basic strength and basicity of produced catalyst. Here, we used a straightforward Hammett indicator titration approach to study all the properties, and the results are shown in Table 6.2. Among the indicators utilised in the titration procedure were bromothymol blue (H_ =7.2), phenolphthalein (H_ =9.8), 2,4-dinitroaniline (H_ =15.0), and 4-nitroaniline (H_ =18.4). 25 mg of catalyst were collected, mixed with 1.0 cm3 of methanol-diluted Hammett indicator solution, and allowed to equilibrate for two hours. After some time, the colour of the indicator solution changed, suggesting that the catalyst is a stronger base than the indicator. By using the Hammett indicator benzene carboxylic acid titration method, the total basicity of the produced catalyst was quantitatively determined. It was found that pure Mg $(NO_3)_2$ has a H_ value between 9.8 and 15.0, making it a moderately weak medium basic site for catalysts. Similar to how the parent compounds, Cu $(NO_3)_3$ and $Mn(NO_3)_3$, which are acidic by nature, did not alter the colour of bromothymol blue. MgO was added to all the salts to increase their fundamental strength. It was discovered that the basic strength of catalysts fell between 15.5 and 18.4 with the addition of MgO. Although the basic strengths of the three catalysts were comparable, $MgMn_2O_4$ (MMO) had the highest number of basic sites (total basicity in units of millimole /g) compared to $MgCu_4O_5$ (CMO) as given in Table 6.1. As transesterification followed a base-catalysed process, MMO's most basic site improved the conversion of glycerol [191].

Table 6.1. Basicity correlation with conversion and yield of the synthesized MMO and CMO.

Catalyst	**Basic Strength**	**Total Basicity (mmol/g)**	**Conversion (%)**	**Yield (%)**
$Mg(NO_3)_2$	9.8-15.0	3.75	27	22
$Mn(NO_3)_2$	9.8-15.0	0.76	9.6	5.4
$Cu(NO_3)_2$	9.8-15.0	0.42	6.7	3.8
$MgCu_4O_5$ (CMO)	15.0-18.4	10.56	83.6	79
$MgMn_2O_4$ (MMO)	15.0-18.4	18.86	97	94

6.4 Evaluation of catalyst for glycerol carbonate synthesis

In the transesterification of glycerol-to-glycerol carbonate using a straightforward reflux condensation procedure, the activity of all the produced catalysts was evaluated. In two separate 200 ml round-bottom flasks, the reaction was conducted using 5.4 mmol of glycerol (5 g) and 16.2 mmol of DMC (14.6 g), respectively. The catalysts $MgMn_2O_4$ and $MgCu_4O_5$ were then added, with the weight percentages of each varying from 1 to 10 wt.% depending on the amount of glycerol used. The reaction mixtures were then heated to the ideal temperature for the ideal amount of time while being continuously stirred. Gas chromatography was used to track the progress of the reactions. Following the reaction method, the result mixtures were

filtered to make it simple to separate the catalyst and continue the investigation in the following reaction process. The liquid mixture's leftover DMC and methanol were also separated using a rotary evaporator. Using gas chromatography (Agilent technology 7890B), the product was found using a capillary column HP-5 (30m 0.32mm 0.25mm) with a flame ionisation detector. For the quantification analysis, tertiary butanol was used as the internal standard. Using the following formulae, the conversion and yield percentages of glycerol and glycerol carbonate were determined.

$$\textbf{Glycerol Conversion (\%)} = \frac{\textbf{No of moles of glycerol reacted}}{\textbf{Total no of moles of glycerol taken}} * \mathbf{100} \qquad \textbf{(6.1)}$$

$$\textbf{Selectivity (\%)} = \frac{\textbf{No of moNo of moles of desired product}}{\textbf{Total no of moles of all products}} * \mathbf{100} \qquad \textbf{(6.2)}$$

$$\textbf{Yield (\%)} = \textbf{\%}\ \mathrm{G}\boldsymbol{lycerol\ conv} \times \%\ \boldsymbol{G}\mathrm{ly}\boldsymbol{C\ selectivity} * \mathbf{100} \qquad \textbf{(6.3)}$$

6.4.1. Gas chromatography analysis of synthesized product glycerol carbonate

The synthesized product was quantified through GC analysis. For the analysis, tert-butanol is used as an internal standard solvent used for the preparation of sample for analysis. After the analysis, it was observed that the retention time of glycerol carbonate was found to be 16.5 min (Figure.6.6). This shows the complete conversion of glycerol-to-glycerol carbonate. The standard gas chromatogram curve of glycerol carbonate lies in the range of 14.90 to 16.50 min retention time and the peak lies at 5.53 retention time depicts the unconverted glycerol.

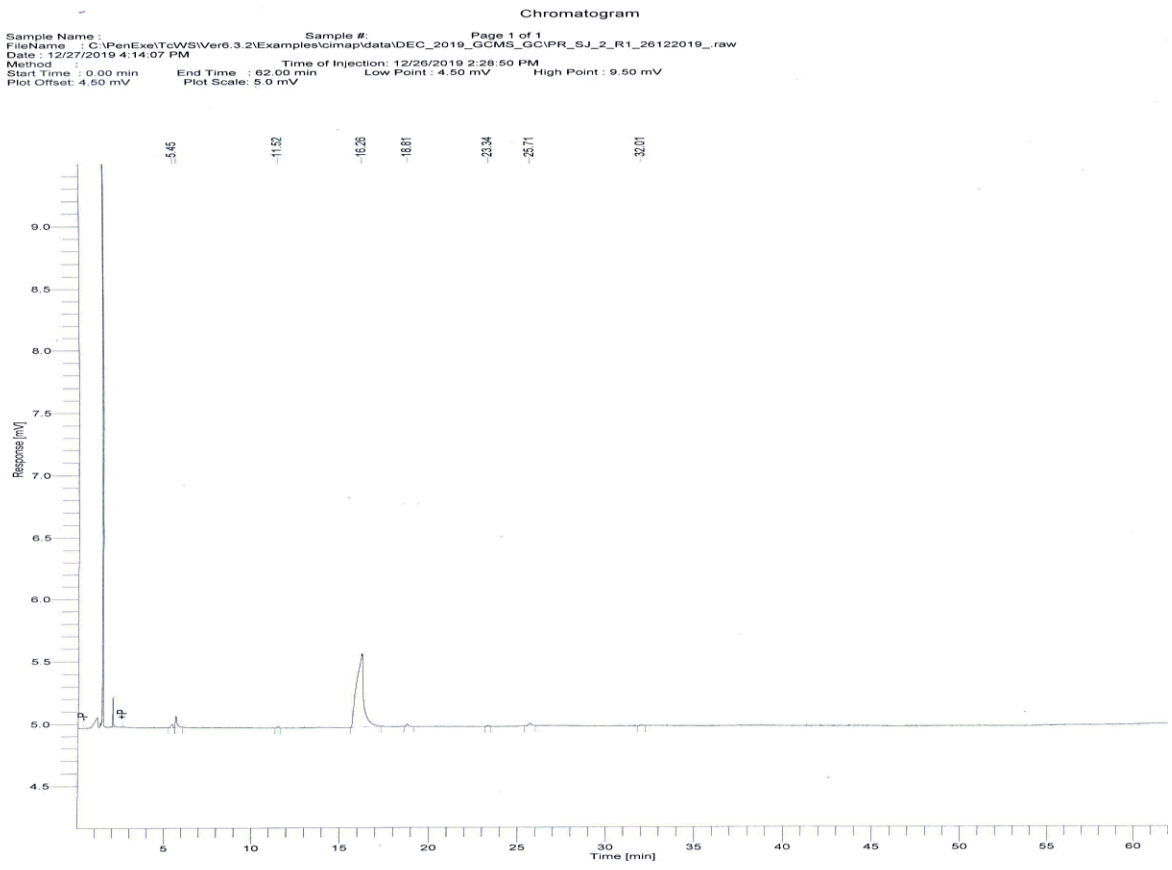

Figure 6.6. GC analysis of glycerol carbonate.

6.5 Detailed study of reaction mechanism in transesterification of glycerol

The primary hydroxyl group of glycerol's primary hydroxyl group is initially abstracted by the Lewis basic site (Mg^{2+}) of the produced MMO catalyst, which is simultaneously activated by the Lewis acidic site (Mn^{4+}), activating the carbonyl carbon of DMC. The resulting generated glyceroxide anion then undergoes nucleophilic addition with activated DMC to create hydroxyl alkyl carbonate while methanol is removed as a by-product. The catalyst is renewed by the cyclization of the unstable intermediate hydroxyl alkyl carbonate, which results in the formation of cyclic glycerol carbonate. Typically, the solid base catalyst serves as a very effective support for the basic site of the catalyst's absorption of H+ from glycerol. Higher basicity of catalyst can increase the more negative charge on glyceroxide anion and therefore

lower the free energy of reaction [192, 193, 194]. The proposed $MgMn_2O_4$ with the highest basicity supports glycerol conversion with the maximum glycerol carbonate yield of 94%.

6.6 Optimization of reaction parameters

6.6.1 Effect of reaction temperature

Temperature, one of the crucial factors in the transesterification of glycerol, was optimised and made clear in Figure 6.7 (a). It was discovered that 90°C produced the highest GlyC yield of 94% and the maximum conversion of glycerol, or 97%. Beyond 90 °C, the conversion of glycerol did not significantly improve, pointing to a high-temperature decarboxylation event that produced glycidol, which was then polymerized by ring-opening [60, 168]. High temperatures also accelerated undesirable processes such as the dehydrogenation and condensation of by-product methanol, which decreased the activity of the catalyst in the conversion of glycerol.

6.6.2 Effect of reaction time

Figure 6.7(b) illustrates the research on the influence of reaction time during glycerol transesterification. When the response time was increased from 25 minutes to 75 minutes, it was found that the reaction obtained the highest conversion of 97%. Glycerol conversion rose from 52 to 97% at 75 minutes. When the duration was increased past 75 minutes, both the conversion and yield of glycerol and GlyC steadily reduced, suggesting that glycerol carbonate had been converted to glycidol. This type of irregularity in GlyC yield and glycerol conversion may be caused by the fact that equilibrium was reached within 75 minutes of the process [140]. 75 minutes was thought to be the ideal reaction time for transesterification of glycerol using this method, depending on the product purity and energy consumption.

6.6.3 Effect of DMC to glycerol molar ratio

The molar ratio of the reactants had a significant impact on the transesterification reaction, as seen in Figure. 6.7(c). It was found that the conversion percentage of glycerol improved from

56 to 97% and the yield percentage of glycerol carbonate likewise increased from 48 to 94% with an increase in the molar ratio of DMC/glycerol from 1:1 to 4:1. The steady decline in glycerol conversion with further DMC to glycerol ratio increases over 4:1 may be caused by the immiscibility of hydrophilic glycerol and hydrophobic DMC at high concentrations, or solubility effect. The rate of reaction slowed down due to the extremely low concentration of glycerol, which is another characteristic that made it difficult to convert glycerol at large DMC:glycerol molar ratios [195].

6.6.4 Effect of catalyst loading

Figure. 6.7(d) illustrates the results of an investigation into the influence of the catalyst amount utilised in the glycerol transesterification procedure. With an increase in catalyst amount up to 5 weight percent of the glycerol employed in the reaction process, the conversion of glycerol increased steadily from 62% to 97%. A rise in the total number of basic sites for catalysts may be the cause of this improvement in the conversion percentage of glycerol. Glycerol conversion was unaffected by further catalyst additions over 5 weight percent, indicating that the catalyst is resistant to the formation of solid-liquid emulsions. The likelihood of pore blockage and a lack of active sites due to particle aggregation at greater catalyst masses is another consideration [101].

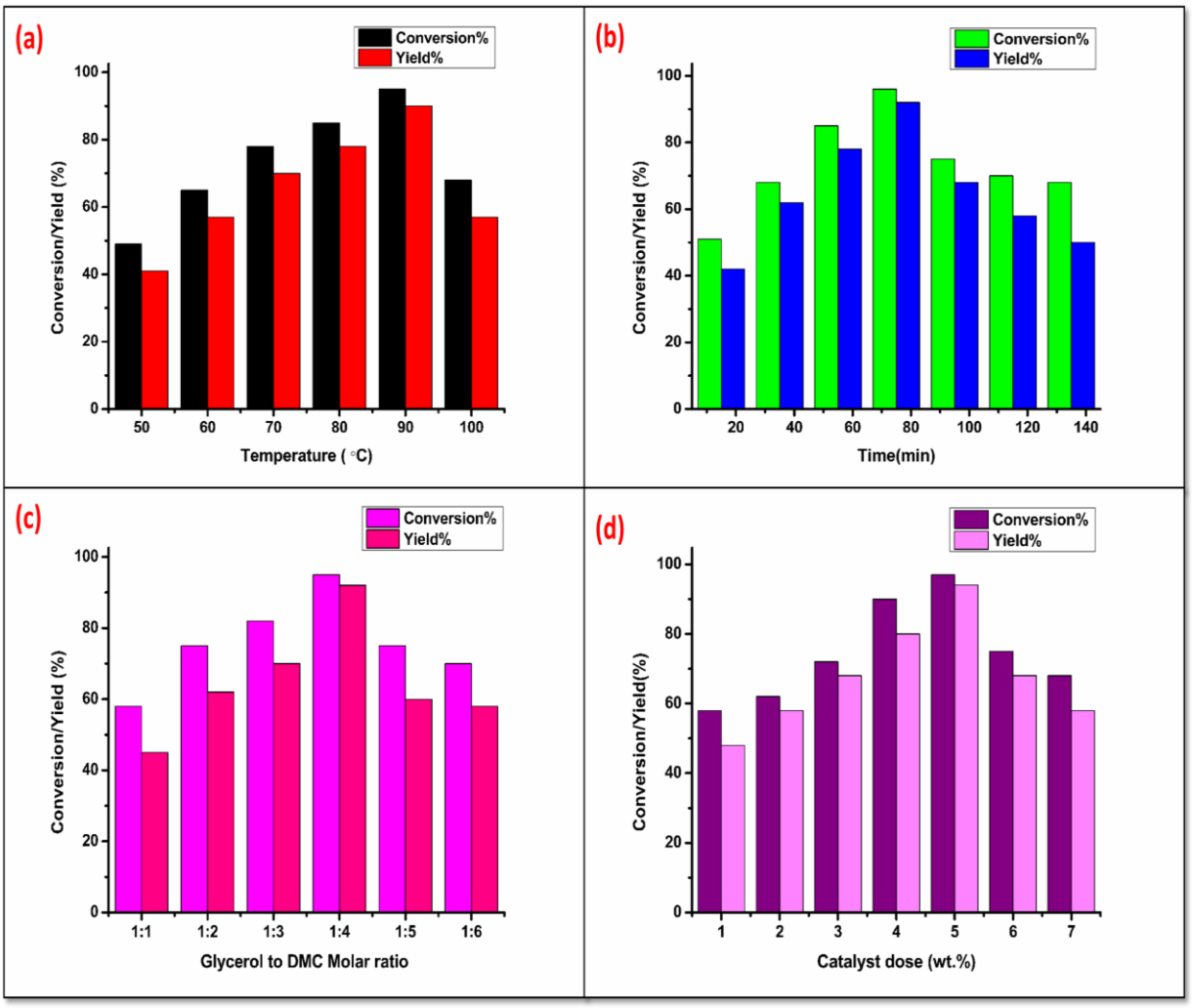

Figure 6.7. Optimization of reaction parameters catalysed by $MgMn_2O_4$ catalyst taking one variable at a time viz., (a) Temp, (b) Time, (c) DMC: Gly molar ratio, (d) Catalyst wt. % on the basis of glycerol used.

6.7. Reusability of catalyst

The stability, activity, and reusability of synthesised catalyst were investigated and are shown in Figure 6.8, which also takes into account the economic and environmental benefits. It was discovered that the catalyst held up well to six cycles of transesterifying glycerol. Leaching tests using a hot filtration approach were used to examine the catalyst's reusability. In this procedure, batch studies were conducted repeatedly. Following each reaction, the catalysts were cleaned thoroughly with methanol before being dried in an oven. Figure 6.8 showed the yield percentage of GlyC and the conversion percentage of Glycerol from preceding

regenerated catalyst. The catalyst is highly effective and can be reused for up to six runs without experiencing a significant loss of activity, according to the results. The well-organized crystallite structure of the catalyst's phase, which aids in stabilising the metallic species of Mg^{2+} and Mn^{4+} as shown by a leaching test, is thought to be responsible for the phenomena of stability of the catalyst up to the sixth runs.

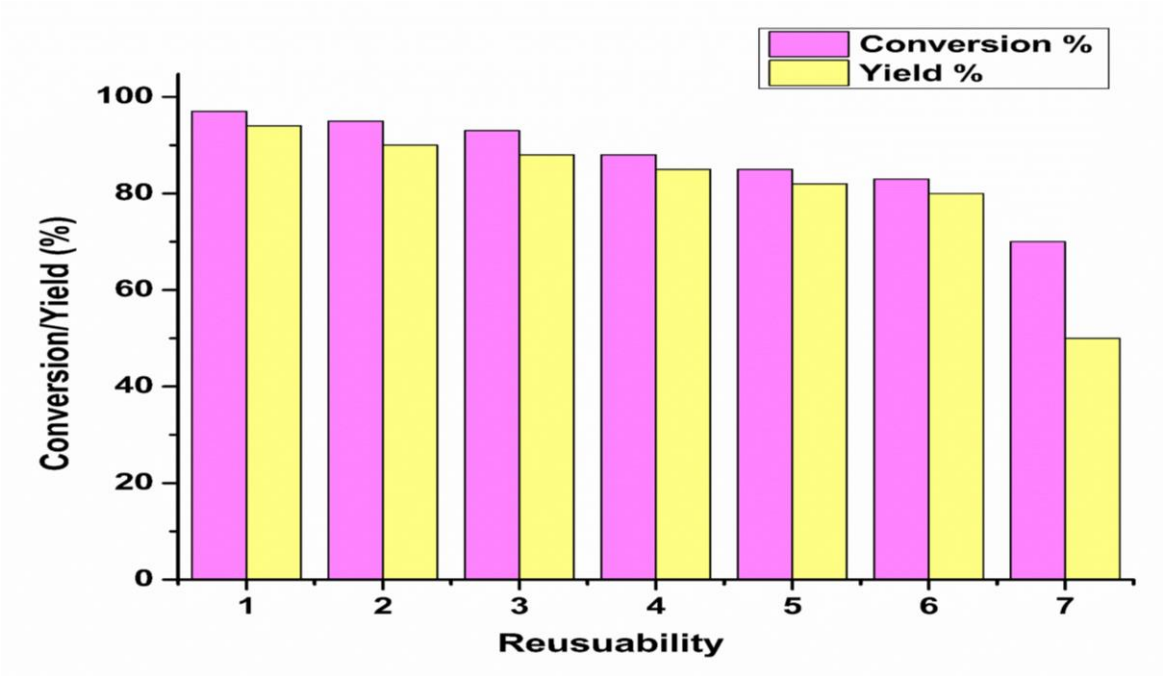

Figure. 6.8 Reusability of MMO catalyst.

6.8. Conclusion

In this study, glycerol waste from the biodiesel industry was used to create glycerol carbonate via a greener process known as transesterification. We were able to successfully synthesise CMO and MMO and investigate their catalytic activity during the transesterification of glycerol. For the transesterification reaction, a comparison between catalysts-like CMO and MMO was done. The full development of the CMO and MMO framework was shown by sophisticated techniques as XRD, TEM-EDX, XPS, FTIR and TGA. All of the characterizations indicated that MMO has greater basic strength, more specific surface area, greater lattice distortion, and smaller particle size than CMO catalyst. All these characteristics of MMO were very helpful for converting glycerol into glycerol carbonate. The presence of manganese in +4 oxidation of Mn in MMO increases the catalytic activity for glycerol transesterification in comparison to CMO. This is another significant factor for the better conversion of glycerol utilising MMO. This signifies the role of support metal in enhancing the activity of catalyst. In order to attain optimal conditions and a higher yield of glycerol carbonate, several reaction parameters were improved. The maximum conversion and yield obtained are 97% and 94.5% respectively. The optimized reaction condition for maximum conversion and yield are 90 reaction temperature, 1:4 glycerol to DMC molar ratio, 5 wt.% of catalyst dose and within 75 min of reaction time produces maximum conversion of glycerol-to-glycerol carbonate.